Materials Science & Engineering A 777 (2020) 139069

Contents lists available at ScienceDirect

Materials Science & Engineering A

journal homepage: http://www.elsevier.com/locate/msea

The activation of deformation mechanisms for improved tensile properties in nanocrystalline aluminum

Sara I. Ahmed [a], K. Andre Mkhoyan [b], Khaled M. Youssef [a,*]

[a] Department of Materials Science and Technology, Qatar University, Doha, 2713, Qatar
[b] Department of Chemical Engineering and Materials Science, University of Minnesota, Minneapolis, 55455, MN, USA

ARTICLE INFO

Keywords:
Nanocrystalline
Aluminum
Tensile properties
Twinning
Dislocations

ABSTRACT

We report tensile properties and TEM observations of in situ consolidated bulk nanocrystalline Al with an average grain size of 29 nm. The nanocrystalline Al is synthesized using a combination of cryogenic and room temperature ball milling. This nanocrystalline Al exhibits extremely high tensile strength, strain hardening rate, and ductility when compared with the conventional coarse-grained commercially pure Al. The tensile strength of this bulk nc Al is at least ten times higher than that of the coarse-grained Al with a total elongation of 10%. These results demonstrate the dependence of the extraordinary tensile properties on the grain size, dislocation activities in the large nanograins, and the deformation twinning controlled by partial dislocations and stacking faults in the nanograins with relatively small grain size.

1. Introduction

Nanocrystalline (nc) metals –with grain sizes < 100 nm– often have unique properties, which are superior to those of their coarse-grained (CG) counterparts [1–4]. Aluminum (Al) is an extremely versatile metal and is considered to be an essential engineering material because of its high specific strength, lightweight, and corrosion resistance. To improve its mechanical properties, several researchers tried to produce Al with grain sizes in the nanoscale range. However, almost all of the reported mechanical properties are obtained for ultra-fine grained (UFG) Al – grain sizes from 100 nm to 1 μm [5–8]. Accordingly, there is a lack of information about the tensile properties of pure bulk nc Al. Additionally, reducing the grain size to the nanoscale range results in extremely high strength, which could trigger unique plastic deformation mechanisms that are not observed in CG materials [9–13]. In the case of nc Al, which has relatively high stacking fault energy, molecular dynamic simulations (MDS) predicted the formation of deformation twinning [14–16]. Twinning was experimentally confirmed in nc Al produced by ball milling [17,18] and nc Al films produced by physical vapor deposition that was exposed to plastic deformation by micro indentation [12]. These studies focused mainly on verifying the presence of twins in nc Al and describing the possible mechanisms of their formation [12,14–21]. However, no report, to the best of our knowledge, described the influence of these deformation twins and other plastic deformation mechanisms on the tensile properties of nc Al. The present study is therefore motivated to synthesize and examine the nanostructure of an artifact-free bulk nanocrystalline Al produced by the in-situ consolidation during milling technique. In particular, this research focuses on the influence of grain size and different deformation mechanisms on the tensile properties of bulk nanocrystalline Al.

2. Experimental procedure

The ball milling of pure Al powder (Alfa Aesar®, 99.99% - 325 mesh) was conducted using a SPEX 8000 shaker mill. The Al powder with a ball-to-powder ratio of 10:1 was loaded into a stainless steel vial in a glovebox under ultra-high purity argon (oxygen level < 0.5 ppm). Synthesizing the artifact-free bulk nanocrystalline Al was then conducted using ball milling at liquid nitrogen and room temperatures. During cryogenic milling, a specially designed Teflon vial was used to hold the stainless steel vial and liquid nitrogen was allowed to flow around the stainless steel vial to maintain its temperature at about 77 K. A PFA Teflon O-ring encapsulating a 302 stainless steel wound ribbon spring (NESAstra Seals®) was used to secure the sealing of the stainless steel vial at low temperatures and prevent nitrogen and oxygen contamination during cryogenic milling. No process control agent was used during ball milling.

The nanostructure of the in situ consolidated spheres was

* Corresponding author. Youssef Department of Materials Science and Technology, Qatar University, Doha, 2713, Qatar.
E-mail address: Kyoussef@qu.edu.qa (K.M. Youssef).

https://doi.org/10.1016/j.msea.2020.139069
Received 28 December 2019; Received in revised form 3 February 2020; Accepted 4 February 2020
Available online 5 February 2020

characterized using an FEI Tecnai G2 transmission electron microscope (TEM) operated at 200 kV. The TEM samples were prepared by using a twin jet electropolishing device (Fischione Model 110) in an electrolytic bath of 10% perchloric acid and 90% ethyl alcohol at ~ 233 K. The fracture surface of the tensile samples was investigated using an FEI Nova NanoSEM scanning electron microscope.

The in-situ consolidated spheres were compacted in a cylindrical tungsten carbide die (inner diameter = 8 mm) and thin discs were sliced from the compacted cylinders using a diamond saw. Several dog-bone shaped tensile specimens were cut from the discs with a gauge length of 3 mm and a width of 1 mm. The surfaces of the specimens were polished to mirror finish and the final thicknesses of the tensile samples ranged from 250 to 370 μm. The tensile tests were performed at ambient temperature using a miniaturized tensile machine with a strain rate of $10^{-3}\,s^{-1}$. Microhardness was measured across the cross-sectional area of the sliced in-situ consolidated spheres using a Future Tech Microhardness Tester, FM-800, equipped with a fully automated hardness testing system (ARS9000). A 25 g load and a loading time of 10 s were utilized during the microhardness indentation process. The hardness results reported in this study is the average of 8 indentations.

3. Results and discussion

In order to synthesize bulk nanocrystalline Al samples, a combination of ball milling at liquid nitrogen and room temperatures was used. The process started by carrying out liquid nitrogen milling for 2 h. Before the cryogenic milling, the sealed stainless steel vial with the loaded Al powder was immersed into liquid nitrogen for 5 min. Then it was placed into the Teflon vial and the liquid nitrogen was allowed to flow continuously around the stainless steel vial during the milling process. After ball milling at liquid nitrogen temperature, the Al powders were welded together to form small rounded agglomerations with about 2–3 mm diameter, see the left image in Fig. 1. *In-situ* consolidation of these rounded agglomerations occurred during the room temperature ball milling. Bulk Al spheres were produced after 6 h of combined milling with sphere diameters up to 6 mm, see the right image in Fig. 1. Chemical analysis was conducted on the *in-situ* consolidated spheres using a laser ablation inductive coupled plasma mass spectroscopy (LA-ICP-MS) technique. The analysis showed oxygen and iron contents of 0.03 wt% and 0.01 wt%, respectively, with no nitrogen contamination. Three spheres were sliced around the center area and mechanically polished for microhardness measurements. No interior voids or pores were observed after slicing the spheres. Additionally, uniform microhardness values were obtained across the polished surfaces of the spheres with an overall average hardness value of 1.1 GPa, see Fig. 1. These results indicate that the consolidated material has identical properties all through the cross-section, confirming the uniformity of the prepared samples, and applicability of the consolidation technique.

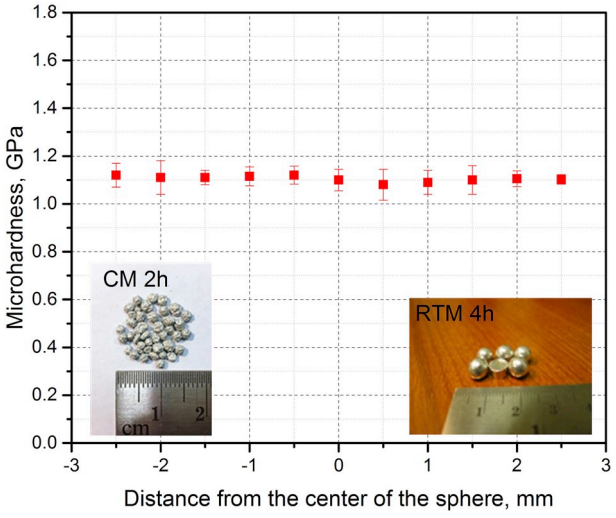

Fig. 1. Vickers microhardness variation across the diameter of the *in-situ* consolidated nc Al spheres. Images of the agglomerated Al pieces after 2 h of cryogenic milling (CM) and the in situ consolidated final spheres after more 4 h of room temperature milling (RTM).

Fig. 2A is a bright-field TEM image of the in situ consolidated nanocrystalline Al samples, which reveals that the sample exhibits grain sizes in the range of 10–55 nm. Statistical analysis of 250 grains shows a monotonic grain size distribution with an average grain size of 29 nm, see Fig. 2B. The TEM observation in Fig. 2A indicates that the nanograins are equiaxed and separated by high-angle grain boundaries with only FCC Al phase present, see the upper right inset of the corresponding selected area diffraction pattern in Fig. 2A. A closer investigation of the nanograins in Fig. 2A shows several planer defects with parallel boundaries that are identified as deformation twins, indicated by arrows

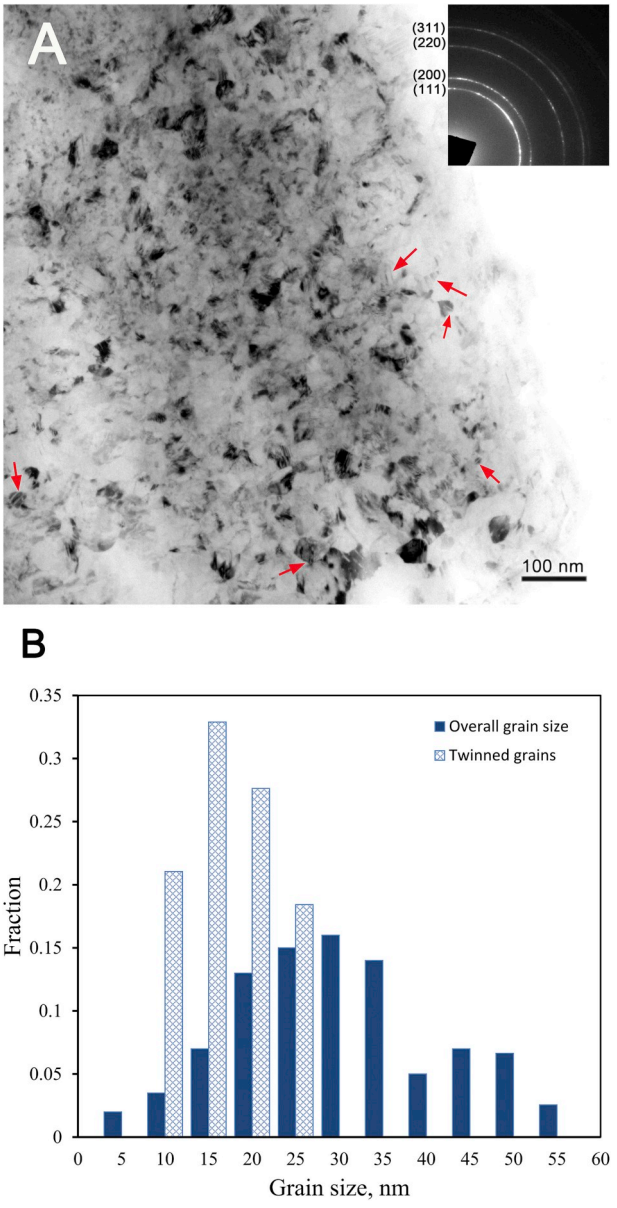

Fig. 2. (A) A bright-field TEM image of consolidated Al after 6 h of combined milling showing nanocrystalline grains with sizes ranging from 10 to 55 nm. The inset, in the upper right corner, is the corresponding selected area diffraction pattern. (B) A statistical grain size distribution of all grains and the grains that contain twins.

in Fig. 2A. Deformation twins have not been observed in single crystal or polycrystalline coarse-grained pure Al subjected to plastic deformation processes with high strain rates such as shock loading even at low temperatures due to its relatively high stacking fault energy [22,23]. However, recent reports showed that a modified dynamic equal channel angular pressing (D-ECAP) technique can provide ultrahigh strain rates ($\sim 10^6$ s^{-1}) and enormous shear strain (200%) to induce macro-deformation twins in single-crystal Al [24]. In the case of nc Al, deformation twins were experimentally observed using plastic deformation techniques with moderate to high strain levels. For instance, the twinning formation was reported in nc Al thin films produced by physical vapor deposition after deformation using either micro indentation or manual grinding [12] and also in nc Al powder that was ball milled in liquid nitrogen with 0.2 wt% stearic acid [17,18]. The deformation twins in the in situ consolidated nc Al (Fig. 2A) seem to form mostly in relatively small nanograins. Forty grains containing twins in the in situ consolidated nc Al were examined and their fraction histogram as a function of the grain size is shown in Fig. 2B. It can be seen from Fig. 2B that the fraction distribution of grains containing twins occurred in small grains (grain size values from 10 to 25 nm). This result confirms the dependency of twinning formation on the grain size in Al that was predicted using molecular dynamics simulations (MDS) by Yamakov et al. [14,15] and also experimentally reported by Chen et al. [12]. An example of these deformation twins is shown in the high-resolution TEM

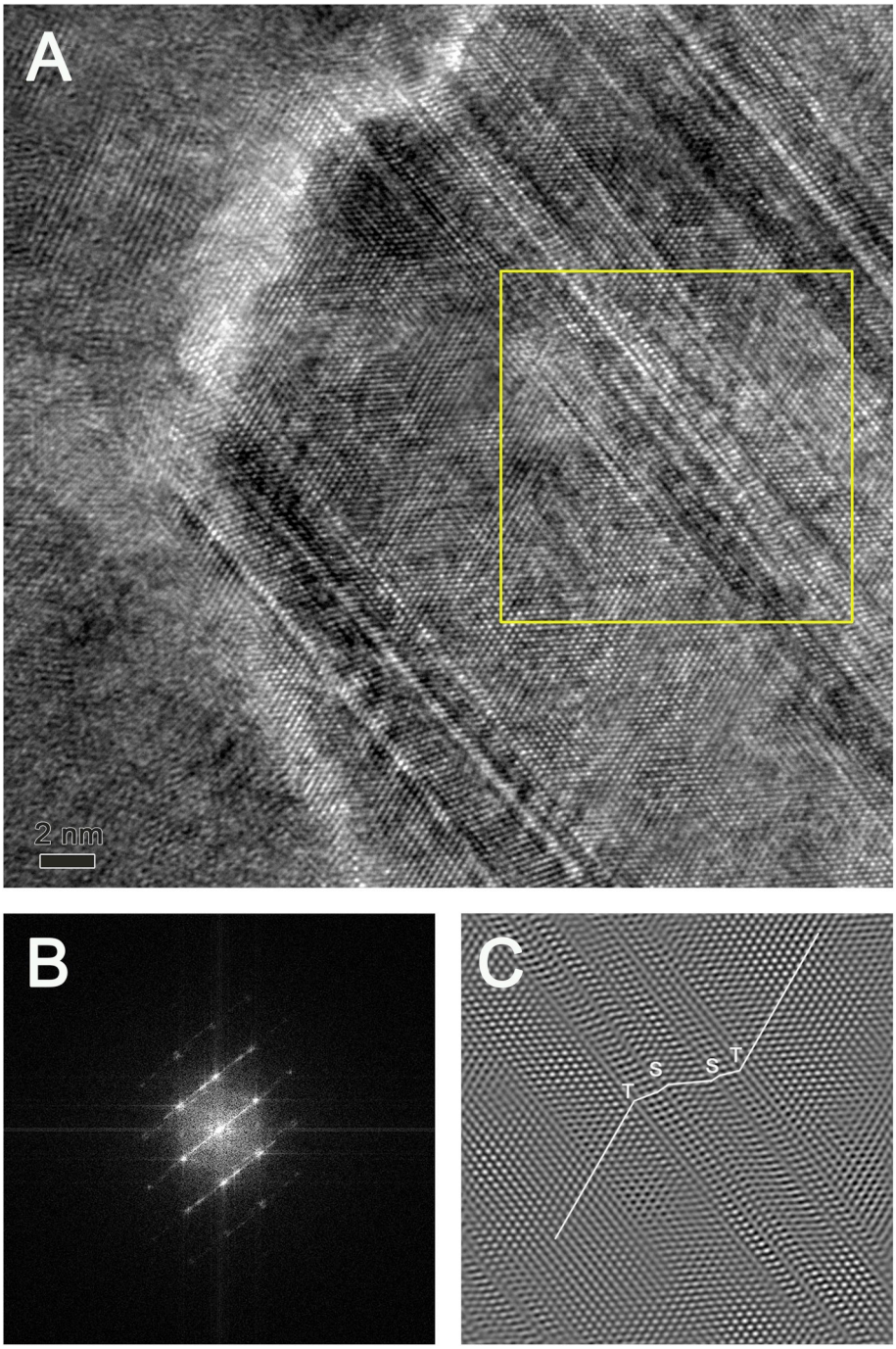

Fig. 3. (A) A high-resolution TEM image of the in situ consolidated nc Al showing a deformation twin with parallel boundaries. (B) A fast Fourier transform pattern of the twinned area in (A). (C) A Fourier-filtered image from the yellow box in (A) showing several deformation twins and stacking faults. (For interpretation of the references to colour in this figure legend, the reader is referred to the Web version of this article.)

image in Fig. 3A with the corresponding fast Fourier transform (FFT) pattern (Fig. 3B). Multiple narrow twin bands residing in a nanograin can be recognized by the mirror symmetry between the twin and the parent lattice. Analysis of these deformation twin boundaries indicates that they are the {111} type. A Fourier-filtered image from the selected area (yellow boxed region in Fig. 3A) shows multiple twins, see Fig. 3C. Several stacking faults and partial dislocations are also observed in the sample.

Several mechanisms of twinning in FCC metals have been proposed and reported [19–21,24–28]. Partial dislocations, which appear to be emitted from the grain boundaries on {111} slip planes, and stacking faults (see Fig. 3C) could facilitate the creation of the deformation twins in our nc Al samples. Chen et al. [12] used the classical dislocation theory in order to evaluate the shear stress needed to activate a full lattice dislocation (τ_L) and a partial dislocation (τ_P) in the nc Al film that was exposed to micro indentation deformation. These shear stresses were described as:

$$\tau_L = \frac{2\eta G b_L}{d} \tag{1}$$

and

$$\tau_P = \frac{2\eta G b_P}{d} + \frac{\gamma}{b_P}, \tag{2}$$

where η is a dislocation characteristic parameter ($\eta = 0.5$ for an edge dislocation and 1.5 for a screw dislocation), G is the shear modulus (35 GPa for Al), γ is the stacking fault energy (160 mJ/m^2 for Al [29]), and b_L and b_P are the Burgers vector magnitudes of full (or lattice) and partial dislocation, respectively. Fig. 4A shows the variation of the critical shear stresses in equations (1) and (2) as a function of the Al grain size, d. It can be seen from Fig. 4A that with decreasing the grain size, τ_P increases with a slower rate than that of τ_L. When the grain size decreases to a critical value (~7 nm in Fig. 4A), τ_P begins to be smaller than τ_L and the activation of partial dislocations becomes easier than that of the lattice dislocation. This finding indicates that twinning could be a preferred deformation mechanism in the small nanograins of the processed Al, which is in agreement with the TEM observations in Figs. 2 and 3. Based on deformation physics and the emission of dislocations from grain boundaries, Zhu et al. [30,31] suggested another analytical model in order to investigate the effect of grain size on the twinning formation of nc FCC metals. In this model, the authors reported a reduction of the twinning shear stress with decreasing the grain size. In the case of nc Al, a minimum critical twinning stress was observed at an average grain size of 6 nm, which is considered by the authors to be an optimum grain size for twinning [30,31]. The statistical analysis of the grains containing twins in the *in-situ* consolidated Al shows that twinning formation occurred in relatively small grains in the range of ~10–25 nm (Fig. 2B). The formation of twins in grains larger than that expected from these analytical models (6–7 nm) could be attributed to the localized stress concentration, the high-stress levels accompanying ball milling, and the influence of elastic anisotropy [20], which were not accounted for in the above models. It is worth mentioning that no twins were observed in grains with size values less than 10 nm. However, the formation of twins in the nanoscale grains on the lower side of the grain size distribution (from 10 to 25 nm, see Fig. 2) is consistent with the experimental observations [30–32] and the results obtained from these models that indicate enabling the deformation by twining as the grain size decreases [12,31].

Tensile testing measurements were conducted at ambient temperature and a strain rate of 10^{-3} s^{-1}. For comparison, similar tensile testing measurements were carried out on annealed commercially pure Al samples. Fig. 4B shows the tensile stress-strain curves of nc Al sample compared to that of the CG Al. The *in-situ* consolidated nc Al exhibits high yield (σ_y at 0.2% offset) and ultimate (σ_u) tensile strengths. The average σ_y of nc Al is found to be as high as 375 MPa and the average σ_u value is 410 MPa. These values are at least ten times higher than those of the conventional coarse-grained Al (see Fig. 4B). The contribution to the strengthening of the *in-situ* consolidated nc Al could result from the grain size refinement. The deformation twins formed in the small nanograin may also affect the obtained high strength. It is well known that twins in coarse-grained or nanostructured materials can affect their mechanical behavior. The twin boundaries act as strong barriers to dislocation motion, which resulted in higher tensile strength. A significant improvement of tensile strength due to twinning was reported in Cu [33,34], Ni [11], and austenitic stainless steel thin films [35]. Possible contribution from contamination to enhance the strength of the in situ consolidated nc Al is neglected since there is no evidence of dispersoids in the results. The yield and ultimate tensile strength values are also higher than those reported for nc Al (53 nm) prepared by active H_2 plasma evaporation technique followed by compaction at high temperatures, $\sigma_y = 257$ MPa and $\sigma_u = 262$ MPa, [38]. Comparable values of σ_y and σ_u were obtained for ultra-fine grained (UFG) Al (commercial purity, 99.9%) with a bimodal distribution of grain sizes that was prepared using ball milling in a liquid nitrogen medium and subsequent extrusion [7]. Even though the grain size of these extruded samples is much larger (> 100 nm) than that of our samples, their high strength was attributed to the presence of different impurities and dispersoids such as Al_2O_3 and

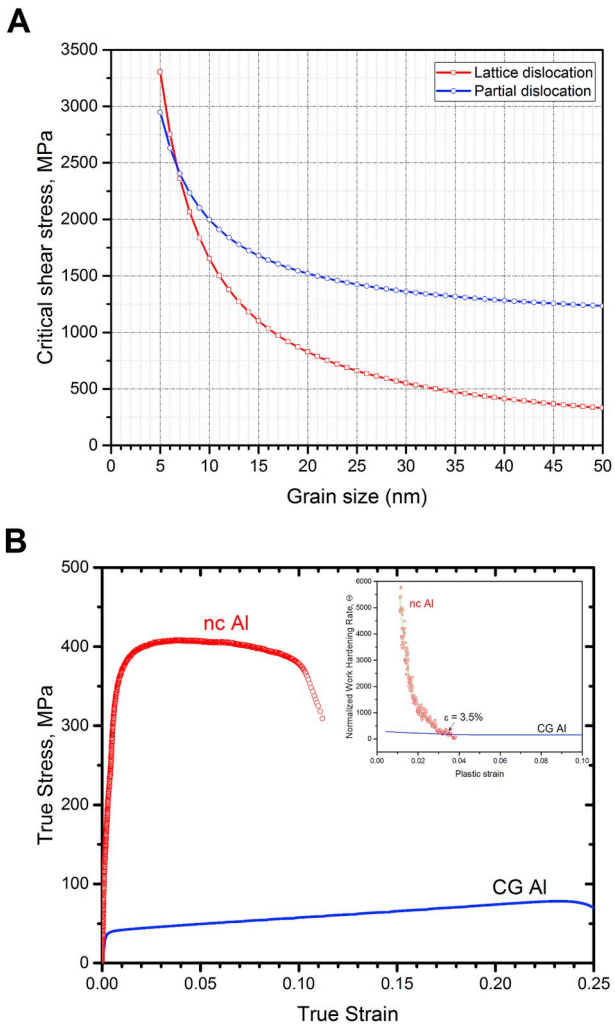

Fig. 4. (A) Critical shear stresses of the lattice and partial dislocations in Al as a function of the grain size calculated from equations (1) and (2). (B) Tensile stress-strain curves for the nc Al and the CG Al. The inset in (B) shows the variation of the strain hardening rate as a function of the true plastic strain for two samples.

AlN.

Combined with the strengthening from the reduced grain size and twining, nc Al exhibits good ductility as well. As illustrated in Fig. 4B, the average uniform and total elongations of the nc Al samples were 4.5% and 10%, respectively. This tensile ductility is higher than that reported by Sun et al. [38] for nanostructured bulk Al samples, which showed a total ductility of 5% and also much higher than that of the nc Al films (22-nm-thick) produced by a sputtering technique that failed with little plastic deformation in tension [39]. This high tensile ductility confirms the integrity of the *in-situ* consolidated nanostructure and the absence of tensile instability and processing artifacts (e.g., pores) that are typically observed in nanocrystalline and UFG materials processed by other techniques [19]. The high tensile ductility observed in Fig. 4B could be attributed to dislocation slip processes during deformation and the activated twins. Several studies reported that deformation twins produced by plastic deformation can significantly enhance the ductility of nanostructured materials [33,36,37].

Another tensile property that also confirms the integrity of the Al nanostructure is the significant strain hardening observed in the stress-strain curve, see Fig. 4B. The strain hardening rate, $\theta = d\sigma/d\varepsilon$, was calculated for the nc Al and the CG Al and plotted as a function of the true plastic strain, see inset in Fig. 4B. It should be noted that nc Al exhibits much higher θ after yielding than CG Al. The strain-hardening exponent, n, of the nc Al was found to be 0.132. Generally, nc bulk materials cannot sustain uniform tensile elongation and show no strain hardening, which causes localized deformation leading to low ductility [39–42]. In the case of UFG Cu and Ni, for example, the nearly zero work hardening rate obtained was attributed to a high pre-existing dislocation density [43]. However, the high θ and n of the in-situ consolidated nc Al indicate a significant dislocation activity during the tensile deformation. In order to further investigate the causes of the observed high θ and the related ductility, a TEM specimen was cut from the surface of the nc Al sample after tensile testing using a focused ion beam (FIB) left-out technique. This TEM specimen was prepared from the middle of the gauge length in the vicinity of the fracture surface. Fig. 5A shows a bright-field TEM image of this sample. It can be seen from Fig. 5A that high dislocation density is observed in the relatively large nanograins. It is worth mentioning that during the room temperature milling to prepare the *in-situ* consolidated nc Al, the temperature of the milling media was detected to be > 65 °C (using a standard Infrared Thermometer Laser Gun). This relatively high temperature could facilitate the dynamic recovery and annihilation of dislocations creating dislocation-free nanograins in these consolidated nc Al. Accordingly, it can be argued that the observed high dislocation density and pile up (Fig. 5A) are generated from the plastic deformation during tensile testing and could be the main reason for the high θ and ductility of the nc Al. SEM image of the fracture surface of the nc Al sample (Fig. 5B) shows a dimpled rupture confirming the dependency of the plastic deformation process on the dislocation activity in the relatively large nanograins. On the other hand, deformation twins are also observed in the nanostructure after tensile testing. The arrows in Fig. 5A point to deformation twins in relatively small nanograins (~20 nm). Even though we cannot confirm whether these twins were formed during the milling process or the tensile plastic deformation, their presence could play a role in the overall strengthening and ductility of the nc Al.

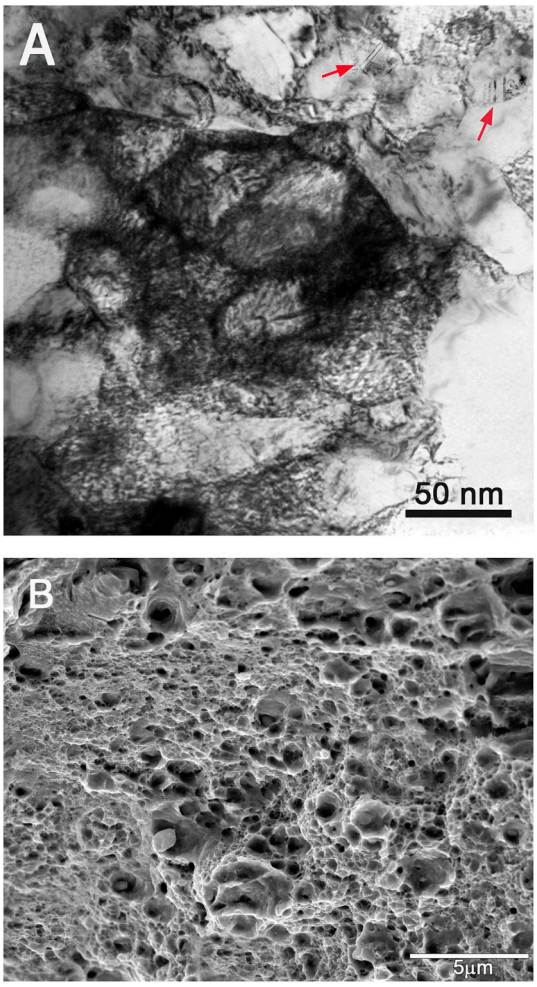

Fig. 5. (A) A bright-field TEM image of the nc Al after tensile testing showing a high density of dislocation and pile-up in the large nanograins and deformations twins in the small nanograins (indicated by red arrows). (B) An SEM image of the nc Al fracture surface. (For interpretation of the references to colour in this figure legend, the reader is referred to the Web version of this article.)

4. Conclusion

In this study, bulk nc Al (29 nm) was synthesized using *in-situ* consolidation during ball milling at liquid nitrogen and room temperatures. The tensile behavior of the nc Al was investigated and correlated with the nanostructure features. Ultra-high yield and ultimate tensile strengths were achieved along with good ductility and strain hardening. The average σ_y of the nc Al samples was found to be as high as 375 MPa and the average σ_u value is 410 MPa. These values are at least ten times higher than those of the conventional CG commercially pure Al. The average uniform and total elongations of the nc Al samples were found to be 4.5% and 10%, respectively. The nc Al exhibited much higher θ after yielding than that of the CG Al with a strain-hardening exponent equals to 0.132. HR-TEM observations showed deformation twins in the nc Al, which became a preferred deformation mechanism in the relatively small nanograins (~10–25 nm). The TEM analysis also showed that partial dislocations, which are emitted from the grain boundaries on {111} slip planes, along with stacking faults could facilitate the creation of these deformation twins. The extremely high strength of the nc Al was attributed to the small grain size and the deformation twinning. TEM observations revealed a high density of dislocations in the large nanograins formed during tensile testing along with deformation twins in the small nanograins, which could be the main reason for high θ and n values that led to good ductility.

Declaration of competing interest

The authors declare that they have no known competing financial interests or personal relationships that could have appeared to influence the work reported in this paper.

CRediT authorship contribution statement

Sara I. Ahmed: Writing - original draft. **K. Andre Mkhoyan:** Formal analysis. **Khaled M. Youssef:** Formal analysis.

Acknowledgment

This work was made possible by NPRP Grant no. NPRP9-180-2-094 from the Qatar National Research Fund (a member of the Qatar Foundation). The statements made herein are solely the responsibility of the authors.

Appendix A. Supplementary data

Supplementary data to this article can be found online at https://doi.org/10.1016/j.msea.2020.139069.

References

[1] C.C. Koch, D.G. Morris, K. Lu, A. Inoue, Ductility of nanostructured materials, MRS Bull. 24 (2) (1999) 54–58.
[2] K.M. Youssef, R.O. Scattergood, K.L. Murty, C.C. Koch, Nanocrystalline Al–Mg alloy with ultrahigh strength and good ductility, Scripta Mater. 54 (2) (2006) 251–256.
[3] J.R. Weertman, D. Farkas, K. Hemker, H. Kung, M. Mayo, R. Mitra, H. Swygenhoven, Structure and mechanical behavior of bulk nanocrystalline materials, MRS Bull. 24 (2) (1999) 44–53.
[4] K.M. Youssef, M.A. Abaza, R.O. Scattergood, C.C. Koch, High strength, ductility, and electrical conductivity of in-situ consolidated nanocrystalline Cu-1% Nb, Mater. Sci. Eng. 711 (2018) 350–355.
[5] C.Y. Yu, P.W. Kao, C.P. Chang, Transition of tensile deformation behaviors in ultrafine-grained aluminum, Acta Mater. 53 (15) (2005) 4019–4028.
[6] N. Kamikawa, T. Hirochi, T. Furuhara, Strengthening Mechanisms in ultrafine-grained and sub-grained high-purity aluminum, Metall. Mater. Trans. 50 (1) (2019) 234–248.
[7] R.W. Hayes, D. Witkin, F. Zhou, E.J. Lavernia, Deformation and activation volumes of cryomilled ultrafine-grained aluminum, Acta Mater. 52 (14) (2004) 4259–4271.
[8] K. Kamikawa, X. Huang, N. Tsuji, N. Hansen, Strengthening mechanisms in nanostructured high-purity aluminium deformed to high strain and annealed, Acta Mater. 57 (14) (2009) 4198–4208.
[9] J. Schiøtz, F.D. Ditolla, K.W. Jacobsen, Softening of nanocrystalline metals at very small grain sizes, Nature 391 (1998) 561–563.
[10] H. Swygenhoven, Grain boundaries and dislocations, Science 296 (5565) (2002) 66–67.
[11] K.S. Kumar, S. Suresh, M.F. Chisholm, J.A. Horton, P. Wang, Deformation of electrodeposited nanocrystalline nickel, Acta Mater. 51 (2) (2003) 387–405.
[12] M. Chen, E. Ma, K.J. Hemker, H. Sheng, Y. Wang, X. Cheng, Deformation twinning in nanocrystalline aluminum, Science 300 (5623) (2003) 1275–1277.
[13] K.M. Youssef, R.O. Scattergood, K.L. Murty, J.A. Horton, C.C. Koch, Ultrahigh strength and high ductility of bulk nanocrystalline copper, Appl. Phys. Lett. 87 (9) (2005), 091904, 091904-3.
[14] V. Yamakov, D. Wolf, S.R. Phillpot, A.K. Mukherjee, H. Gleiter, Dislocation processes in the deformation of nanocrystalline aluminium by molecular-dynamics simulation, Nat. Mater. 1 (1) (2002) 45–48.
[15] V. Yamakov, D. Wolf, S.R. Phillpot, H. Gleiter, Deformation twinning in nanocrystalline Al by molecular-dynamics simulation, Acta Mater. 50 (20) (2002) 5005–5020.
[16] B. Li, B.Y. Cao, K.T. Ramesh, E. Ma, A nucleation mechanism of deformation twins in pure aluminum, Acta Mater. 57 (15) (2009) 4500–4507.
[17] X.Z. Liao, F. Zhou, E.J. Lavernia, S.G. Srinivasan, M.I. Baskes, D.W. He, Y.T. Zhu, Deformation mechanism in nanocrystalline Al: partial dislocation slip, Appl. Phys. Lett. 83 (4) (2003) 632–634.
[18] X.Z. Liao, F. Zhou, E.J. Lavernia, D.W. He, Y.T. Zhu, Deformation twins in nanocrystalline Al, Appl. Phys. Lett. 83 (24) (2003) 5062–5064.
[19] M.A. Meyers, A. Mishra, D.J. Benson, Mechanical properties of nanocrystalline materials, Prog. Mater. Sci. 51 (4) (2006) 427–556.
[20] Y.T. Zhu, X.Z. Liao, X.L. Wu, Deformation twinning in bulk nanocrystalline metals: experimental observations, JOM 60 (9) (2008) 60–64.
[21] L. Wang, P. Guan, J. Teng, P. Liu, D. Chen, W. Xie, D. Kong, S. Zhang, T. Zhu, Z. Zhang, E. Ma, M. Chen, X. Han, New twinning route in face-centered cubic nanocrystalline metals, Nat. Commun. 8 (1) (2017), 2142.
[22] K.W. Jacobsen, J. Schiøtz, Computational materials science: nanoscale plasticity, Nat. Mater. 1 (1) (2002) 15–16.
[23] G.T. Gray III, J.C. Huang, Influence of repeated shock loading on the substructure evolution of 99.99 wt.% aluminum, Mater. Sci. Eng. 145 (1) (1991) 21–35.
[24] F. Zhao, L. Wang, D. Fan, B.X. Bie, X.M. Zhou, T. Suo, Y.L. Li, M.W. Chen, C.L. Liu, M.L. Qi, M.H. Zhu, S.N. Luo, Macrodeformation twins in single-crystal aluminum, Phys. Rev. Lett. 116 (2016), 075501.
[25] J.A. Venables, Deformation twinning in face-centered cubic metals, Philos. Mag. A 6 (63) (1961) 379–396.
[26] R.J. Asaro, P. Krysl, B. Kad, Deformation mechanism transitions in nanoscale fcc metals, Phil. Mag. Lett. 83 (12) (2003) 733–743.
[27] X.Z. Liao, Y.H. Zhao, S.G. Srinivasan, Y.T. Zhu, Deformation twinning in nanocrystalline copper at room temperature and low strain rate, Appl. Phys. Lett. 84 (4) (2004) 592–594.
[28] H. Rösner, J. Markmann, J. Weissmüller, Deformation twinning in nanocrystalline Pd, Phil. Mag. Lett. 84 (5) (2004) 321–334.
[29] J.P. Hirth, J. Lothe, Theory of Dislocations, Wiley, New York, 1982.
[30] Y.T. Zhu, X.Z. Liao, S.G. Srinivasan, Y.H. Zhao, E.J. Lavernia, Nucleation and growth of deformation twins in nanocrystalline aluminum, Appl. Phys. Lett. 85 (2004), 5049.
[31] Y.T. Zhu, X.Z. Liao, X.L. Wu, J. Narayan, Grain size effect on deformation twinning and detwinning, J. Mater. Sci. 48 (2013) 4467–4475.
[32] WuXL, Y.T. Zhu, Phys. Rev. Lett. 101 (2008), 025503.
[33] L. Lu, Y.F. Shen, X.H. Chen, L.H. Qian, K. Lu, Ultrahigh strength and high electrical conductivity in copper, Science 304 (2004) 422–425.
[34] K. Lu, L. Lu, S. Suresh, Strengthening materials by engineering coherent internal boundaries at the nanoscale, Science 324 (2009) 349–352.
[35] X. Zhang, A. Misra, H. Wang, M. Nastasi, J.D. Embury, T.E. Mitchell, Nanoscale-twinning-induced strengthening in austenitic stainless steel thin films, Appl. Phys. Lett. 84 (2004), 1096.
[36] Y.H. Zhao, Y.T. Zhu, X.Z. Liao, Z. Horita, T.G. Langdon, Tailoring stacking fault energy for high ductility and high strength in ultrafine-grained Cu and its alloy, Appl. Phys. Lett. 89 (2006), 121906.
[37] Y.H. Zhao, J.E. Bingert, X.Z. Liao, B.Z. Cui, K. Han, A.V. Sergueeva, Simultaneously increasing the Ductility and strength of ultra-fine-grained pure copper, Adv. Mater. 18 (2006), 2949.
[38] X.K. Sun, H.T. Cong, M. Sun, M.C. Yang, Preparation and mechanical properties of highly densified nanocrystalline Al, Metall. Mater. Trans. 31 (3) (2000) 1017–1024.
[39] M.A. Haque, M.T. Saif, Mechanical behavior of 30–50 nm thick aluminum films under uniaxial tension, Scripta Mater. 47 (12) (2002) 863–867.
[40] D. Jia, K.T. Ramesh, E. Ma, Failure mode and dynamic behavior of nanophase iron under compression, Scripta Mater. 42 (1) (1999) 73–78.
[41] D. Jia, Y.M. Wang, K.T. Ramesh, E. Ma, Deformation behavior and plastic instabilities of ultrafine-grained titanium, Appl. Phys. Lett. 79 (5) (2001) 611–613.
[42] T.R. Malow, C.C. Koch, P.Q. Miraglia, K.L. Murty, Compressive mechanical behavior of nanocrystalline Fe investigated with an automated ball indentation technique, Mater. Sci. Eng. 252 (1) (1998) 36–43.
[43] G.T. Gray, T.C. Lowe, C.M. Cady, R.Z. Valiev, I.V. Aleksandrov, Influence of strain rate & temperature on the mechanical response of ultrafine-grained Cu, Ni, and Al-4Cu-0.5Zr, Nanostruct. Mater. 9 (1–8) (1997) 477–480.